Materials Letters 64 (2010) 1462–1464

Contents lists available at ScienceDirect

Materials Letters

journal homepage: www.elsevier.com/locate/matlet

Surface modification of $Ca_{60}Mg_{15}Zn_{25}$ bulk metallic glass for slowing down its biodegradation rate in water solution

H.F. Li [a,b], Y.B. Wang [a,b], Y. Cheng [c], Y.F. Zheng [a,b,c,*]

[a] State Key Laboratory for Turbulence and Complex System, College of Engineering, Peking University, Beijing 100871, China
[b] Department of Advanced Materials and Nanotechnology, College of Engineering, Peking University, Beijing 100871, China
[c] Center for Biomedical Materials and Tissue Engineering, Academy for Advanced Interdisciplinary Studies, Peking University, Beijing 100871, China

ARTICLE INFO

Article history:
Received 1 February 2010
Accepted 22 March 2010
Available online 30 March 2010

Keywords:
Metals and alloys
Thin film
Deposition
Wettability
Corrosion behavior
Ca–Mg–Zn bulk metallic glass

ABSTRACT

Three kinds of new barrier films were introduced on the surface of $Ca_{60}Mg_{15}Zn_{25}$ bulk metallic glasses (BMGs) in order to slow down its biodegradation/corrosion rate, including fluoroalkylsilane (FAS) coating, pure Fe film and (Fe + FAS) bilayer. The changes of surface morphology were characterized by scanning electron microscopy (SEM). Contact angle meter was applied to test the surface wettability at ambient temperature. The corrosion rate was investigated by immersion test in deionized water. It was found that various micro-nanoscale hierarchical structures could be constructed after different surface treatments. By suitable surface modification strategy, $Ca_{60}Mg_{15}Zn_{25}$ BMG showed increased water contact angle even up to 133.6°. The immersion experiment results showed that Fe film and FAS thin film coatings with hydrophobic and insulative characteristics are beneficial to provide effective anti-corrosive protection to $Ca_{60}Mg_{15}Zn_{25}$ BMG, with the sequence: Fe coating > (Fe + FAS) treated > FAS treated.

1. Introduction

Much interest has been drawn upon the study of BMGs in the past decades due to their outstanding physical, mechanical and chemical properties. Recently Fe-based [1] and Mg-based BMGs [2] had been investigated by the present authors as potential biomaterials with excellent corrosion resistance and acceptable biocompatibility. Among various BMG materials, Ca–Mg–Zn BMGs are much more attractive with unique properties, such as low density (~2.0 g/cm^3) and low Young's modulus close to the modulus of human bones [3]. The most important thing is that Ca–Mg–Zn BMG can degrade in water solution, which makes it perfect as biodegradable bone tissue engineering scaffold material, with a combination of satisfactory mechanical properties and biological-friendly constituents, since (1) there are about 1000–1500 g Ca in an adult human body [4]; (2) Mg is helpful for calcium incorporation into the bone [5]; (3) Zinc can stimulate fracture healing of bone, reduce postmenopausal bone loss, improve bone mineralization and skeletal strength [6].

Unfortunately bare Ca–Mg–Zn BMG is too bioreactive in the body solution, and its degradation rate is too fast to be tolerated by human body before its functional retirement. Although amorphous Ca–Mg–Zn exhibited better anti-oxidation properties than in crystalline conditions[7], earlier works showed that destructive and fast corrosion could happen to CaMgZn glassy alloy in static aqueous environment with a corrosion penetration rate of 5691 + 1046 μm/year, and only non-protective compounds formed on the surfaces [8–10]. In order to decrease its degradation rate, it is necessary to fabricate coatings onto the surface of Ca–Mg–Zn BMG. Pure Fe has been recently developed as biodegradable materials, with its corrosion products being non-toxic and a relatively slow degradation rate [11]. Liu et al. [12] used Fluoroalkylsilane (FAS) coating to construct superhydrophobic surface on Mg-based alloy and found that it could dramatically improve corrosion resistance of the Mg-based alloy.

So, in the present study, three kinds of biodegradable films were introduced on the surface of $Ca_{60}Mg_{15}Zn_{25}$ BMG, including fluoroalkylsilane (FAS) coating, pure Fe film and (Fe + FAS) bilayer, aiming to slow down its degradation rate.

2. Materials and methods

The Ca-based BMGs, with nominal composition of $Ca_{60}Mg_{15}Zn_{25}$ (at.%) (hereafter abbreviated as CMZ) were fabricated by induction melting of the pure elements (99.9 wt.% in purity) in an argon atmosphere. The prepared alloys were induction remelted and were injected into a water-cooled copper mold with a cavity of 15 mm × 15 mm × 2 mm. CMZ plates with 5 mm × 5mmm × 2 mm were cut by a low speed diamond saw. Fe film, about 100 nm thick, was coated on CMZ substrate by magnetron sputtering of pure Fe (99.5 wt.%) metal using a radio-frequency magnetron sputtering (RFMS) equipment. Before FAS modification, CMZ plates were etched by water with different times (15 min and 30 min). Then the water-

* Corresponding author. Postal Address: Department of Advanced Materials and Nanotechnology, College of Engineering, Peking University, Beijing 100871, China. Tel./fax: +86 10 6276 7411.
E-mail address: yfzheng@pku.edu.cn (Y.F. Zheng).

0167-577X/$ – see front matter © 2010 Elsevier B.V. All rights reserved.
doi:10.1016/j.matlet.2010.03.060

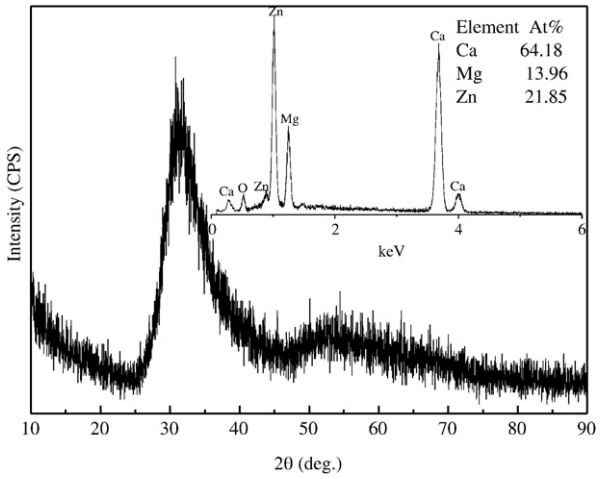

Fig. 1. XRD pattern and EDS spectrum (inset) of untreated $Ca_{60}Mg_{15}Zn_{25}$ BMG.

etched CMZ samples were rinsed with acetone, dried in air, then immersed in a 1.0% ethanol solution of FAS ($CF_3(CF_2)_7CH_2CH_2Si(OCH_3)_3$) for 48 h, and subsequently heated at 50 °C for 2 h.

X-ray diffractometer (Rigaku DMAX 2400) using CuKα radiation was employed for the identification of the amorphous structure of as-prepared CMZ samples, and the actual chemical composition was analyzed by energy-disperse spectrometer (EDS). Changes in the surface morphologies and the microstructures of the samples before and after surface modification were characterized by scanning electron microscope(Hitachi S-4800), equipped with EDS attachment. The water contact angle was measured using a Dataphysics OCA20 contact angle system. An average of three measurements was taken for each sample. The immersion test was carried out in deionized water and the temperature was kept at 37 °C using a water bath. The amount of hydrogen generation was measured in accordance to Ref. [13] during the immersion test. An average of three measurements was taken for each group.

3. Results and discussion

3.1. XRD and EDS analysis

Fig. 1 shows the XRD pattern of untreated CMZ sample. There is no diffraction peak corresponding to crystalline phases, indicating the amorphous state of the CMZ sample. From the EDS analysis, it can be seen that the composition of the as-prepared CMZ was very close to its nominal composition.

3.2. Surface characteristics

Typical SEM images of CMZ samples after different surface modification are shown in Fig. 2, with insets showing high magnification images of randomly-selected single papillae. It can be seen that with prolonging the water etching time from 15 min to 30 min, randomly distributed papillae in micrometer size range (Fig. 2(a)–(b)) were formed, the number and the size of which increased and the morphology changed from peony-like morphology to gengon-like morphology with multi-protuberance. After further treatment by FAS solution, the surface papillae of water-etched CMZ samples transform into angular fuzzy because of the wrapping effect of FAS (Fig. 2(c)–(d)). The resultant CMZ possess a rough surface with micro-nanoscale hierarchical structure, which was believed to be very important for the formation of high water contact angle [12,14]. Additionally as can be seen in Fig. 2(e), after deposition of biodegradable pure Fe film, there was no obvious change on the surface topography of CMZ sample, yet the resulting surface layer shows loosened morphology with further FAS treatment (Fig. 2(f)).

The corresponding water contact angle of the CMZ samples with different surface modifications are presented in Fig. 3. After water etching for different times, the contact angle of the CMZ sample does not increase substantially, which means that the surface active nature of CMZ sample still remains. However, after FAS modification, the water contact angles of CMZ samples increase dramatically, correspondingly the wettability changes from hydrophilic to hydrophobic. Meanwhile, it is also interesting to notice that "30 min water etching + FAS" CMZ sample has a significant improvement in comparison to "15 min water etching + FAS" treated one, which might be related to the difference of their surface roughness. For Fe coated CMZ sample, the contact angle increases to some degree comparing to the untreated one, but is not as large as FAS-treated one. Among all samples, Fe + FAS coating shows the largest contact angle value, indicating a strong hydrophobic feature.

3.3. Corrosion behavior

Fig. 4 shows the hydrogen generation tendency of CMZ during immersion in deionized water before and after different surface modification. It can be seen that the average hydrogen generation rate (0.5195 ml $cm^{-2}h^{-1}$) for FAS treated sample is much less than that

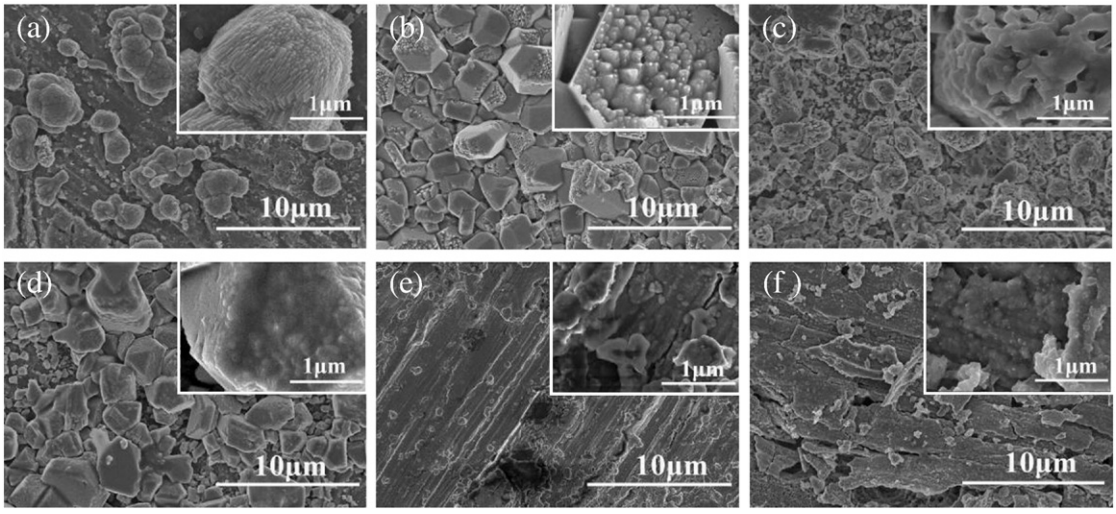

Fig. 2. Surface topography of CMZ samples after different surface treatment: (a) 15 min water etching; (b) 30 min water etching; (c) 15 min water etching + FAS; (d) 30 min water etching + FAS; (e) Fe coating; (f) Fe + FAS coating.

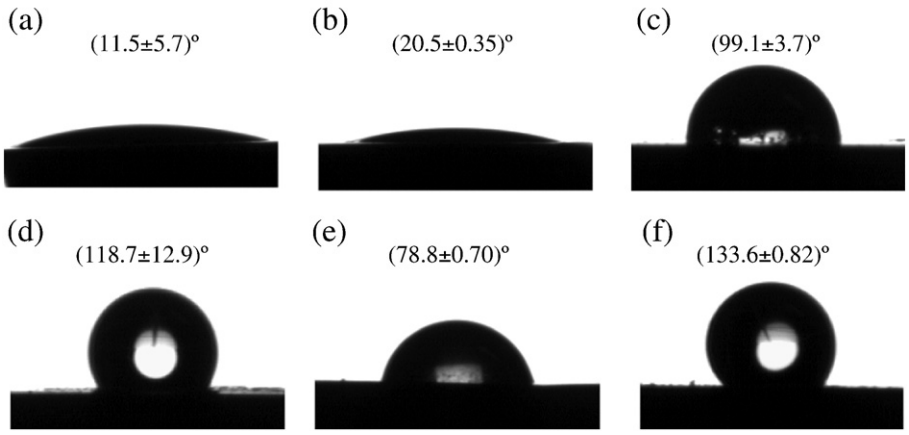

Fig. 3. Contact angle of CMZ after different surface modification: (a) 15 min water etching; (b) 30 min water etching; (c) 15 min water etching + FAS; (d) 30 min water etching + FAS; (e) Fe coating; (f) Fe + FAS coating.

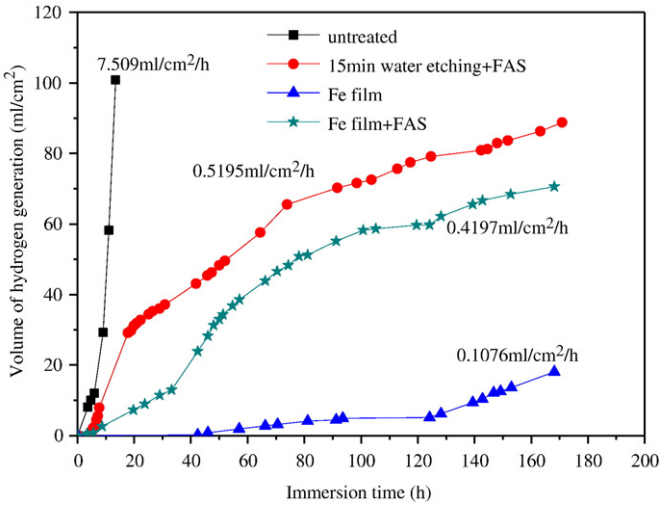

Fig. 4. The hydrogen generation volumes of CMZ before and after surface modification.

of untreated sample ($7.509\ ml\ cm^{-2}h^{-1}$), indicating that the corrosion rate of CMZ is reduced significantly as a result of low surface free energy [12,14]. Among all samples, Fe coated CMZ shows the best corrosion resistance, since there is almost no H_2 releasing for the first 48 h, and the average hydrogen generation rate is only $0.1076\ ml\ cm^{-2}h^{-1}$. Although showing the highest contact angle, the corrosion rate of "Fe coated + FAS" CMZ sample increased to $0.4197\ ml\ cm^{-2}h^{-1}$, due to its loosen surface layer structure. However, "Fe + FAS bilayer film" is still more protective in comparison to the untreated sample and the "water etching + FAS" film.

4. Conclusions

Based on the above results, the following conclusions can be made. (1) After water etching, different micro-nanoscale hierarchical structures could be obtained on the surface of $C_{60}Mg_{15}Zn_{25}$ BMG, that is, peony-like shapes for 15 min etching; pinboard-like shape for 30 min etching. (2) With FAS treating, the edges and corners are all smoothed compared to only water etching effect, besides, the water contact angle increased and the corrosion-resistance was improved significantly for $Ca_{60}Mg_{15}Zn_{25}$ BMG. (3) Among these surface modification techniques, the sequence of corrosion rate from high to low was: untreated>F AS>Fe + FAS>Fe film. (4) Surface modification methods, especially with the Fe coating, are quite effective to control the corrosion behavior of $C_{60}Mg_{15}Zn_{25}$ BMG, which makes this BMG possible for further biomedical application as biodegradable metallic materials.

Acknowledgements

This work was supported by the National Natural Science Foundation of China (No. 30770580) and National Basic Research Program of China (973 Program) with Grant No. 2007CB936103.

References

[1] Wang YB, Li HF, Cheng Y, Wei SC, Zheng YF. Electrochem Comm 2009;11:2187–90.
[2] Gu XN, Zheng YF, Zhong SP, Xi TF, Wang JQ, Wang WH. Biomaterials 2010;30:1093–103.
[3] Senkov ON, Miracle DB, Scott JM. Intermetallics 2006;14:1055–60.
[4] Ilich JZ, Kerstetter JE. J Am Coll Nutr 2000;19:715–37.
[5] Li ZJ, Gu XN, Lou SQ, Zheng YF. Biomaterials 2008;29:1329–44.
[6] Yamaguchi M. J Trace Elem Exp Med 1998;11:119–35.
[7] Barnard BR, Liaw PK, Buchanan RA, Senkov ON, Miracle DB. Mater Trans JIM 2007;48:1870–8.
[8] Dahlman J, Senkov ON, Scott JM, Miracle DB. Mater Trans JIM 2007;48:1850–4.
[9] Morrison ML, Buchanan RA, Senkov ON, Miracle DB, Liaw PK. Metall. Mater Trans A 2006;37:1239–45.
[10] Senkov ON, Miracle DB, Keppens V, Liaw PK. Metall. Mater Trans A 2008;39:1888–900.
[11] Peuster M, Hesse C, Schloo T, Fink C, Beerbaum P, Schnakenburg C. Biomaterials 2006;27:4955–62.
[12] Liu KS, Zhang ML, Zhai J, Wang J, Jiang L. Appl Phys Lett 2008;92(183103):1–3.
[13] Song GL, Atrens A. Adv Eng Mater 2003;5:837–58.
[14] Zhao K, Liu KS, Li JF, Wang WH, Jiang L. Scripta Mater 2009;60:225–7.